

Synthesis and Characterization of Manganese Sulphide Thin Films by Chemical Bath Deposition Method

G. GEETHA^a, P. MURUGASEN^b AND S. SAGADEVAN^{c,*}

^aResearch Scholar, Bharathiar University, Coimbatore, India

^bDepartment of Physics, Saveetha Engineering, Chennai-600 123, India

^cCentre for Nanotechnology, AMET University, Chennai-603 112, India

(Received November 10, 2015; revised version August 30, 2017; in final form September 15, 2017)

Manganese sulphide (MnS) thin films were prepared by chemical bath deposition method. X-ray diffraction analysis was used to study the structure and the crystallite size of MnS thin films. The grain size and the surface morphology were studied using scanning electron microscopy. The optical properties were studied using the UV-visible absorption spectrum. The dielectric properties of MnS thin films were studied for different frequencies and different temperatures. Further, electronic properties, such as valence electron plasma energy, average energy gap or the Penn gap, the Fermi energy and electronic polarizability of the MnS thin films were calculated. The ac electrical conductivity study revealed that the conduction depended both on the frequency and the temperature. The temperature dependent conductivity study confirmed the semiconducting nature of the films.

DOI: [10.12693/APhysPolA.132.1221](https://doi.org/10.12693/APhysPolA.132.1221)

PACS/topics: MnS thin films, XRD, SEM, dielectric studies

1. Introduction

The deposition of materials in the form of thin film has been the subject of intensive research over the past decades due to applications in various fields such as antireflection coatings and optical filters, surface acoustic wave devices, electronic components (both discrete and integrated), fabrication of large area photodiode arrays, solar selective coatings, solar cells, photoconductors, sensors, etc. The chemical deposition methods are low cost processes and the films are found to be of quality comparable with those obtained by more sophisticated and expensive physical deposition process. Among these chemical methods, chemical bath deposition (CBD) which falls in the solution growth categories, controlled precipitation, or simply chemical deposition, has emerged recently as the most popular method for the deposition of metal chalcogenide thin films [1]. The CBD method is presently attracting considerable attention, as it does not require sophisticated instrumentation like vacuum system and other expensive equipments. Simple equipments like hot plate with magnetic stirrer are needed. The starting chemicals are commonly available and cheap. Metal chalcogenide thin film preparation by CBD is currently receiving a lot of attention as it is relatively inexpensive, simple and convenient for large area deposition. A variety of substrates such as insulators, semiconductors or metals can be used, since it is a low temperature process which avoids oxidation or corrosion of metallic substrates. It is a slow process which facilitates better orientation of crystallites with improved grain structure. In recent years, chalcogenide films of different metals have

attracted much attention due to their potential applications in solar cells as a window/buffer material, as well as in sensors, photoconductors, optical mass memories, etc. Manganese sulphide (MnS) is an important semiconductor material because of its interesting properties such as direct band gap, abundance in nature and absence of toxicity. Thus, manganese sulfide thin films have been widely used in a variety of applications such as solar cells, solar selective coatings, sensors, photoconductors, optical mass memories and antireflection coating [2–4]. Several methods have been applied to obtain manganese sulfide thin films such as radio-frequency sputtering, hydrothermal, SILAR and chemical bath deposition [5–8].

In this paper the authors deposited MnS thin films on glass substrates by CBD technique. The CBD deposited MnS thin films were characterized by X-ray diffraction (XRD), scanning electron microscopy (SEM), UV-vis analysis and dielectric variation with temperature techniques.

2. Experimental procedure

All the starting chemicals utilized in this investigation were of 99.5% analytical grade, commercially available and were used without further purification. The substrate cleaning is very important in the deposition of thin films. Commercially available glass slides were washed using soap solution and subsequently kept in hot chromic acid and then cleaned with deionized water followed by rinsing in acetone. Finally, the substrates were ultrasonically cleaned with deionized water for 10 min and wiped with acetone and stored in a hot oven at 40 °C. MnS thin films were prepared on commercial microscopic glass slide by using the CBD technique. In typical procedure, firstly 20 ml of 1 M manganese acetate tetrahydrate ($C_4H_6MnO_4 \cdot 4H_2O$) and 4 ml of 7.4 M triethanolamine ($C_6H_{15}NO_3$) (TEA) were vigorously mixed in 100 ml

*corresponding author; e-mail: sureshsagadevan@gmail.com

glass beaker for 5 min. After that, 20 ml of 1.5 M ammonia solution (NH_4OH) was added to the solution and further stirred for 10 min. Then under constant stirring, 0.4 ml of hydrazine hydrate ($\text{H}_4\text{N}_2\text{H}_2\text{O}$) (80%) solution was mixed followed by 20 ml of 1.4 M thioacetamide ($\text{C}_2\text{H}_5\text{NS}$) and the solution was stirred for 10 min. The final solution was made 75 ml by adding double distilled water. The pH of the bath solution was found to be 11. The already cleaned micro-scope glass slides were used as substrates. The glass slide substrate was immersed in the prepared bath solution and kept vertical in the beaker for thin film deposition. The deposition was done at room temperature. After 6 h, the glass slide was removed, rinsed with double distilled water and allowed air drying. Many trials were conducted to optimize the deposition parameters to obtain a good quality MnS thin film. The resultant films were homogeneous and well adhered to the substrate with mirror like surface. The deposited good quality MnS thin films were subjected to characterization studies. The XRD pattern of the MnS thin films was recorded by using a powder X-ray diffractometer Shimadzu model: XRD 6000 using $\text{Cu } K_\alpha$ radiation, in the diffraction angle range of 0° and 80° . The crystallite size was determined from the broadenings of corresponding X-ray spectral peaks by using the Scherrer formula. SEM studies were carried out on JEOL, JSM-67001. The optical absorption spectrum of the MnS thin films was obtained by using the VARIAN CARY MODEL 5000 spectrophotometer in the wavelength range of 300–900 nm. The dielectric properties of the MnS thin films were analyzed using a HIOKI 3532-50 LCR HITESTER over the frequency range 50 Hz–5 MHz.

3. Results and discussion

3.1. X-ray diffraction analysis

The phase composition and the structure of the film were studied by X-ray diffraction analysis. The XRD pattern of MnS thin film is shown in Fig. 1. The XRD peaks could be indexed as (111), (200), (211), (102), (110), (103), (004), and (202). The observed peaks corresponded to the formation of cubic phase of MnS and therefore were indexed according to cubic structure. Knowing the wavelength λ , full width at half maximum (FWHM) of the peaks β , and the diffracting angle θ , the particle size D was calculated by using the Scherrer formula

$$D = 0.9\lambda / (\beta \cos \theta). \quad (1)$$

Using the above relation, the average size of the MnS was found to be ≈ 34 nm.

3.2. SEM analysis

SEM was used for studying the surface morphology and the micro structural features of the as deposited MnS thin films. SEM image was obtained for MnS thin film deposited on glass substrate in order to study thin film surface. Figure 2 shows the SEM image of the MnS thin films. Microstructural studies revealed the formation of morphological features, with mostly spherical shape being detected in the MnS thin films.

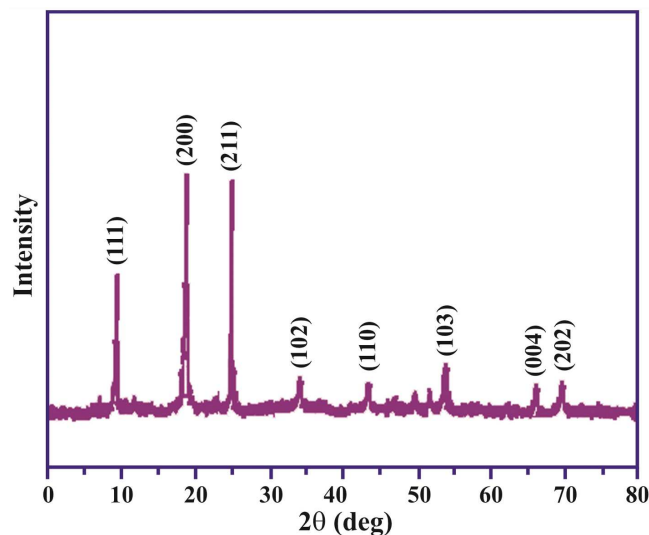


Fig. 1. XRD spectrum of MnS thin films.

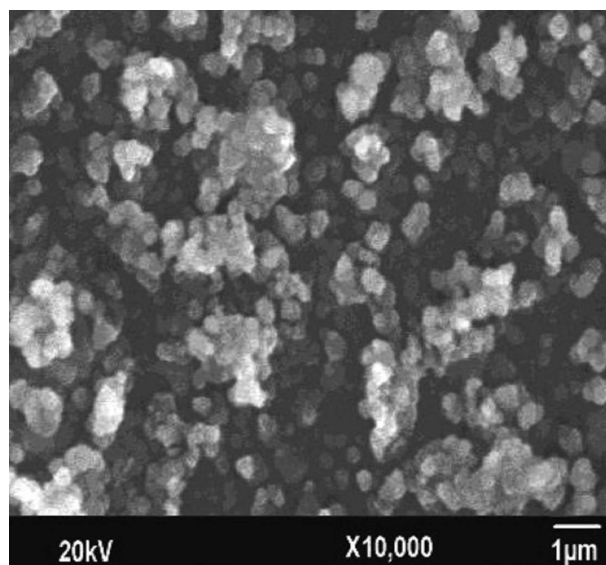


Fig. 2. SEM image of the MnS thin films.

3.3. Optical studies

Optical properties are very significant as far as applications in any optoelectronic devices are concerned. Optical band gap and absorption coefficient are two important parameters of a solar cell material. In the present study, optical characterization was done for the determination of the nature of absorption spectrum and the energy band gap of MnS thin films. The optical absorption spectrum of the MnS thin films deposited onto the glass slides were studied in the wavelength range of 300–900 nm and it is shown in Fig. 3. The spectrum indicates that the strong absorption is found at shorter wavelength region while weak absorption is observed at the longer wavelength region. The dependence of optical absorption coefficient on photon energy helps to analyze the type of band structure and the optical transition. The optical absorption coefficient α was calculated from transmittance using the

following relation:

$$\alpha = \frac{1}{d} \log \left(\frac{1}{T} \right), \quad (2)$$

where T is the transmittance and d is the thickness of the film. The fundamental absorption corresponding to the optical transition of the electrons from the valence band to the conduction band can be used to determine the nature and value of the optical band gap E_g of the films. As a direct band gap material, the film under study has an absorption coefficient α obeying the following relation for high photon energies ($h\nu$) and can be expressed as

$$\alpha = \frac{A(h\nu - E_g)^{1/2}}{h\nu}, \quad (3)$$

where E_g is the band gap of the as-deposited MnS thin film and A is a constant. A plot of variation of $(\alpha h\nu)^2$ versus $h\nu$ is shown in Fig. 4. Using the Tauc plot, the optical bandgap (E_g) was obtained as 3.30 eV which is almost similar to the reported value 3.23 eV [9].

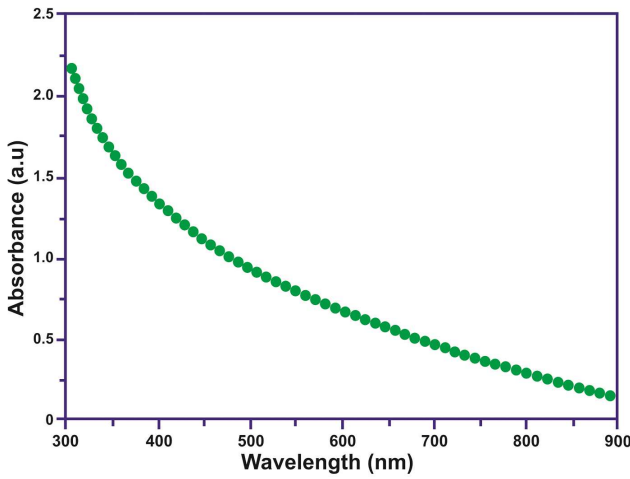


Fig. 3. UV-visible absorption spectrum of MnS films.

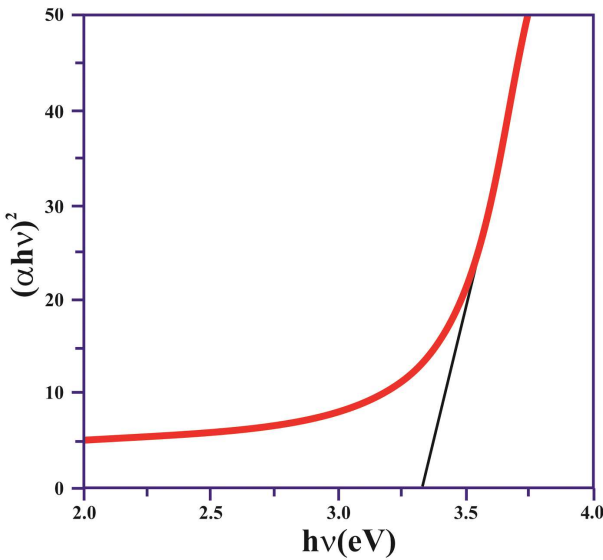


Fig. 4. Plot of $(\alpha h\nu)^2$ vs. photon energy ($h\nu$).

3.3.1. Determination of optical constants

Two of the most important optical parameters, namely the refractive index n and the extinction coefficient K are generally called optical constants. The amount of light that transmits through thin film material depends on the amount of the reflection and the absorption that take place along the light path. The optical constants such as the refractive index n , the real dielectric constant ε_r and the imaginary part of dielectric constant ε_i were calculated. The extinction coefficient K was determined using the following equation [10]:

$$K = \frac{\lambda\alpha}{4\pi}. \quad (4)$$

The extinction coefficient (K) was found to be 0.005 at $\lambda = 900$ nm. The transmittance (T) is given by

$$T = \frac{(1 - R)^2 \exp(-\alpha t)}{1 - R^2 \exp(-2\alpha t)}. \quad (5)$$

Reflectance R in terms of absorption coefficient can be obtained from the above equation.

Hence we have

$$R = \frac{1 \pm \sqrt{1 - \exp(-\alpha t) + \exp(\alpha t)}}{1 + \exp(-\alpha t)}. \quad (6)$$

The refractive index n can be determined from the reflectance data using the following equation:

$$n = -\frac{(R + 1) \pm \sqrt{3R^2 + 10R - 3}}{2(R - 1)}. \quad (7)$$

The refractive index n was found to be 1.68 at $\lambda = 900$ nm. The high refractive index enables MnS film to become suitable for use in optoelectronic devices. From the optical constants, electrical susceptibility (χ_c) could be calculated using the following relation:

$$\varepsilon_r = \varepsilon_0 + 4\pi\chi_c = n^2 - k^2. \quad (8)$$

Hence we have

$$\chi_c = \frac{n^2 - k^2 - \varepsilon_0}{4\pi}, \quad (9)$$

where ε_0 is the permittivity of free space. The obtained value of the electrical susceptibility (χ_c) of as-deposited MnS thin film was 1.82 at $\lambda = 900$ nm. Since electrical susceptibility is greater than 1, the material can be easily polarized when the incident light is more intense. The real part of the dielectric constant ε_r and the imaginary part of the dielectric constant ε_i was calculated using the following relations:

$$\varepsilon_r = n^2 - k^2, \quad (10)$$

$$\varepsilon_i = 2nk. \quad (11)$$

The values of the real dielectric constant ε_r and the imaginary dielectric constant ε_i at $\lambda = 900$ nm were estimated to be 2.35 and 0.042, respectively.

3.4. Dielectric studies

The dielectric constant was analyzed as a function of the frequency at different temperatures as shown in Fig. 5, while the corresponding dielectric loss is shown in Fig. 6. The dielectric constant could be evaluated using the relation

$$\varepsilon_r = \frac{Cd}{\varepsilon_0 A}, \quad (12)$$

where C is the capacitance, d is the thickness of the films, ε_0 is the permittivity of free space, and A is the area of the films. The film thickness is measured using a Surfcom 480A (Tokyo Seimitsu) profilometer. The dielectric constant with frequency for various temperatures is shown in Fig. 5. It is observed (Fig. 5) that the dielectric constant decreases exponentially with increasing frequency and then attains almost a constant value in the high frequency region. The analysis of the plot shows that the value of the dielectric constant increases with an increase in the temperature. The large value of the dielectric constant is due to the fact that MnS thin films act as a nanodipole under electric fields [11]. The dielectric loss studied as a function of frequency at different temperatures is shown in Fig. 6. These curves suggest that the dielectric loss is largely dependent on the frequency of the applied field, similar to that of the dielectric constant. The dielectric loss decreases with an increase in the frequency at almost all temperatures, but appears to achieve saturation in the higher frequency range at all the temperatures [12]. In the low frequency region, high energy loss is observed, which may be due to the dielectric polarization, space-charge and rotation-direction polarization occurring in the low frequency range [13, 14].

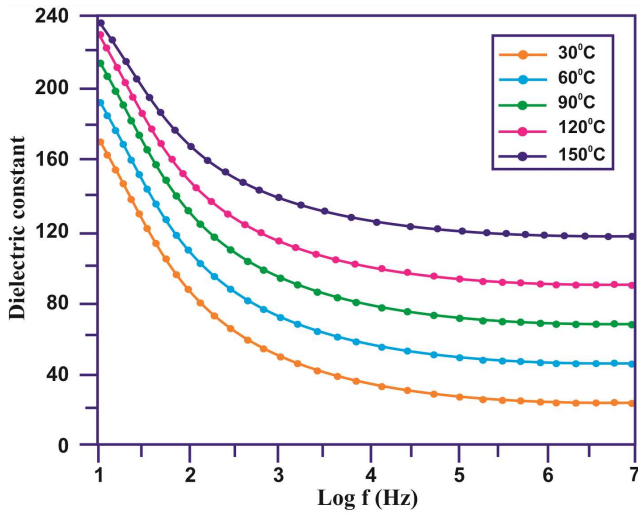


Fig. 5. Dielectric constant of MnS thin films.

The high frequency dielectric constant is required as input to evaluate electronic properties like valence electron plasma energy, average energy gap or the Penn gap, the Fermi energy and electronic polarizability of the MnS thin films. The theoretical calculations showed that the high frequency dielectric constant was explicitly dependent on the valence electron. Plasma energy, an average energy gap referred to as the Penn gap and Fermi energy. The Penn gap was determined by fitting the dielectric constant with the plasmon energy [15]. The following relation was used to calculate the valence electron plasma energy ω_p :

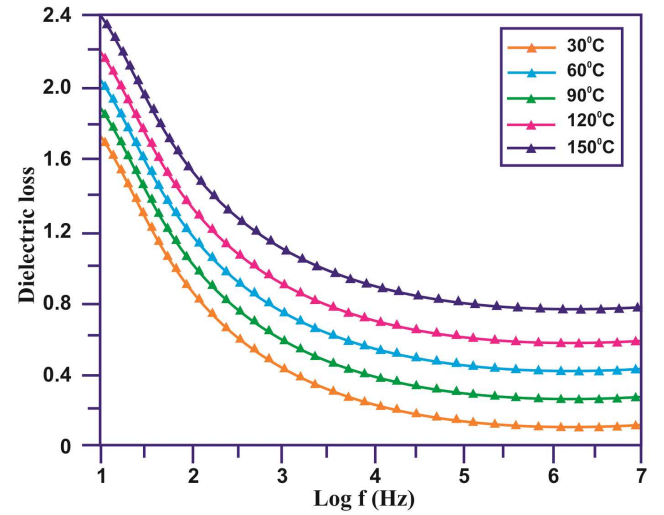


Fig. 6. Dielectric loss of MnS thin films.

$$\hbar\omega_p = 28.8\sqrt{Z\rho/M}. \quad (13)$$

According to the Penn model [16], the average energy gap for the MnS thin films is given by

$$E_p = \frac{\hbar\omega_p}{\sqrt{\varepsilon_\infty - 1}}, \quad (14)$$

where $\hbar\omega_p$ is the valence electron plasmon energy and the Fermi energy is given by

$$E_F = 0.2948(\hbar\omega_p)^{4/3}. \quad (15)$$

Then, the electronic polarizability α , is obtained using the relation [17]:

$$\alpha = 0.396 \times 10^{-24} \frac{(\hbar\omega_p)^2 S_0}{(\hbar\omega_p)^2 S_0 + 3E_p^2} \frac{M}{\rho} [\text{cm}]^3, \quad (16)$$

where S_0 is a constant given by

$$S_0 = 1 - \frac{E_p}{4E_F} + \frac{1}{3} \left(\frac{E_p}{4E_F} \right)^2. \quad (17)$$

The Clausius–Mossotti relation also gives α [18]:

$$\alpha = \frac{3M}{4\pi N_\alpha \rho} \frac{\varepsilon_\infty - 1}{\varepsilon_\infty + 2}. \quad (18)$$

The following empirical relationship is also used to calculate α :

$$\alpha = 0.396 \times 10^{-24} \left(1 - \frac{\sqrt{E_g}}{4.06} \right) \frac{M}{\rho} [\text{cm}]^3, \quad (19)$$

where E_g is the band gap value determined through the UV-visible spectrum. The high frequency dielectric constant of the materials is a very important parameter for calculating the physical/electronic properties of materials. All the above parameters as estimated are tabulated in Table I.

The electronic polarizability of the MnS thin films is thus found to be related to the energy gap by the above relation. As can be seen in Table I, the agreement between the calculated values of α using relations (16) and (19) is very good. Relation (19) should therefore prove useful in an estimation of the electronic polarizability directly from the energy gap of the semiconductor [18]. It is

TABLE I

Electronic parameters of the MnS thin films.

Parameter (method)	Value
plasma energy $h\omega_p$	10.56 eV
Penn gap E_p	2.32 eV
Fermi energy E_F	3.47 eV
electronic polarizability (Penn analysis)	$4.52 \times 10^{-24} \text{ cm}^3$
electronic polarizability (Clausius–Mossotti relation)	$4.92 \times 10^{-24} \text{ cm}^3$
electronic polarizability (bandgap)	$4.57 \times 10^{-24} \text{ cm}^3$

interesting to investigate the relationship between energy gap (E_g) and electron polarizability α [19]. Hence, manganese sulfide (MnS) is a magnetic semiconductor material ($E_g = 3.30 \text{ eV}$) that is of potential interest in short wavelength optoelectronic applications such as in solar selective coatings, solar cells, sensors, photoconductors, optical mass memories.

3.5. AC electrical conductivity studies

The conductivity of a material depends on its overall characteristics such as its chemical composition, purity, and crystal structure. Measurements taken with continuous currents provide only total conductivity. In the present study, electrical ohmic contacts were made using air drying silver paint on the opposite faces. Electrical measurements were taken in the frequency range 50 Hz to 5 MHz using HIOKI 3532-50 LCR HITESTER. A chromel-alumel thermocouple was employed to record the sample temperature. A 30 min interval was used prior to thermal stabilization after each measuring temperature. All the measurements were carried out in atmospheric air. The temperature dependent ac electrical conductivity study was carried out. The temperature dependent ac conductivity of the MnS thin films is shown in Fig. 7. It is observed that the conductivity σ_{ac} increases with an increase in the temperature and the frequency [20]. The electrical conductivity as a function of inverse of temperature of as deposited MnS films is shown in Fig. 8. The temperature dependence on resistance is expressed as

$$R = R_0 \exp(-E_a/kT), \quad (20)$$

where E_a is the thermal activation energy, k is the Boltzmann constant and T is the temperature in absolute scale. The activation energy is obtained using the relation

$$\sigma = \sigma_0 \exp(-\Delta E_a/kT), \quad (21)$$

where σ is the carrier conductivity. The activation energy of the MnS thin films was found to be 0.28 eV.

4. Conclusion

The MnS thin films were prepared by the chemical bath deposition technique. The XRD studies revealed a well crystallized and cubic phase and the crystallite size were

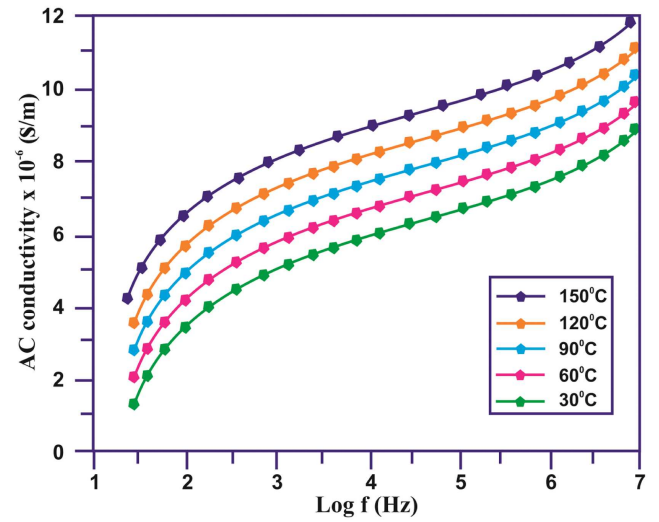


Fig. 7. Variation of conductivity with log frequency.

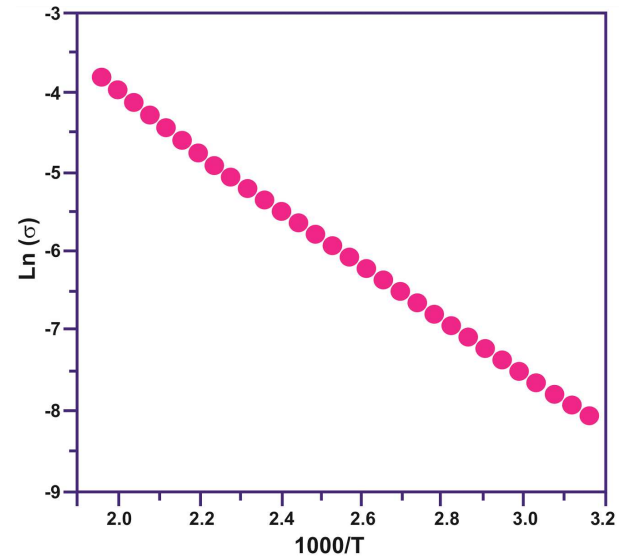


Fig. 8. Variation of conductivity with log frequency.

found to be 34 nm of the MnS thin films. The morphology of the MnS thin films were characterized by using SEM. The UV-visible spectrum showed excellent transmission in the entire visible region. The optical properties such as band gap, refractive index, extinction coefficient, and electrical susceptibility were calculated to analyze the optical property. The optical band gap was found to be 3.30 eV. The dielectric constant and the dielectric loss of the MnS thin films were calculated for different frequencies and temperatures. In addition, the plasma energy of the valence electron, the Penn gap or average energy gap, the Fermi energy, and electronic polarizability of the MnS thin films were also determined. The ac electrical conductivity was found to increase with an increase in the temperature and the frequency. The activation energy was found to be 0.28 eV.

References

- [1] S.H. Chaki, S.M. Chauhan, J.P. Tailor, M.P. Deshpande, *J. Mater. Res. Technol.* **6**, 123 (2017).
- [2] D. Fan, X. Yang, H. Wang, Y. Zhang, H. Yan, *Physica B* **337**, 165 (2003).
- [3] D. Sreekantha Reddy, D. Raja Reddy, B. Reddy, A. Mallikarjuna Reddy, K. Gunasekhar, P. Sreedhara Reddy, *J. Optoelectron. Adv. Mater.* **9**, 2019 (2007).
- [4] S. Agbo, F. Ezema, *Pacific J. Sci. Technol.* **8**, 150 (2007).
- [5] A. Hannachi, S. Hammami, N. Raouafi, H. Maghraoui-Meherzi, *J. Alloys Comp.* **663**, 507 (2016).
- [6] Y. Zhang, H. Wang, B. Wang, H. Yan, M. Yoshimura, *J. Cryst. Growth* **243**, 214 (2002).
- [7] H. Pathan, S. Kale, C. Lokhande, S. Han, O. Joo, *Mater. Res. Bull.* **42**, 1565 (2007).
- [8] C. Gumus, C. Ulutas, R. Esen, O. Ozkendir, Y. Ufuktepe, *Thin Solid Films* **492**, 1 (2005).
- [9] Dong Bo Fan, Hao Wang, Yong Cai Zhang, Jie Cheng, Hui Yan, *Surf. Rev. Lett.* **11**, 27 (2004).
- [10] S. Sagadevan, J. Podder, *Soft Nanosci. Lett.* **5**, 55 (2015).
- [11] S. Sagadevan, *J. Non-Oxide Glasses* **6**, 47 (2014).
- [12] G. Geetha, P. Murugasen, S. Sagadevan, *Mater. Res.* **19**, 413 (2016).
- [13] S. Thirumavalavan, K. Mani, S. Sagadevan, *J. Ovonic Res.* **11**, 123 (2015).
- [14] G. Geetha, P. Murugasen, S. Sagadevan, *Mater. Res.* **20**, 62 (2017).
- [15] N.M. Ravindra, R.P. Bharadwaj, K. Sunil Kumar, V.K. Srivastava, *Infrared Phys.* **21**, 369 (1981).
- [16] D.R. Penn, *Phys. Rev.* **128**, 2093 (1962).
- [17] N.M. Ravindra, V.K. Srivastava, *Infrared Phys.* **20**, 67 (1980).
- [18] M. Ravindran, V.K. Srivastava, *Infrared Phys.* **19**, 605 (1979).
- [19] S. Ahmad, M. Ashraf, A. Ahmad, D.V. Singh, *Arab. J. Sci. Eng.* **38**, 1889 (2013).
- [20] S. Thirumavalavan, K. Mani, S. Sagadevan, *Chalcogenide Lett.* **12**, 237 (2015).